Journal of Peptide Science, Vol. 2, 3–13 (1996)

Elucidation of the Structure of Constrained Bicyclopeptides in Solution by Two-dimensional Cross-relaxation Spectroscopy: Amatoxin Analogues

CARLA ISERNIA[1], LUCIA FALCIGNO[2], SLOBODAN MACURA[3], LIVIO PAOLILLO[2], ANNA LISA PASTORE[4] and GIANCARLO ZANOTTI[5]

[1] Second University of Naples, Environmental Sciences Faculty, Caserta, Italy
[2] Department of Chemistry, University of Naples, Naples, Italy
[3] Department of Biochemistry and Molecular Biology, Mayo Graduate School, Mayo Foundation, Rochester, Minnesota, USA
[4] European Molecular Biology Department, Heidelberg, Germany
[5] Centro Studi Chimica del Farmaco, CNR, University of Rome, Italy

Received 11 May 1995
Accepted 21 July 1995

Abstract: The evaluation of peptide structures in solution is made feasible by the combined use of two-dimensional NMR in the laboratory (NOESY) and rotating frames (ROESY), and by the use of molecular dynamics calculations. The present paper describes how both the NMR method and molecular dynamics calculations were applied to very rigid synthetic bicyclic peptides that are analogues of natural amatoxins. The NMR theory, which allows the estimate of interatomic distances between interacting nuclei, is briefly discussed. The experimental data were compared with those of known solid-state structures. Three amatoxin analogues have been examined. Of these, one is biologically active (*S*-deoxo γ[R] OH-Ile^3-amaninamide) and its structure in the solid state has recently been worked out. The second and third analogues (*S*-deoxo-Ile^3-Ala^5-amaninamide and *S*-deoxo-D-Ile^3-amaninamide, respectively) are inactive and their solid-state structures are unknown. The data presented confirm the authors' previous hypothesis that lack of biological activity of *S*-deoxo-Ile^3-Ala^5-amaninamide is due to the masking of the tryptophan ring by the methyl group of L-Ala and not to massive conformational changes of the analogue.

Keywords: Structure of amatoxin analogues; constrained bicyclopeptides; NMR; molecular dynamics

INTRODUCTION

The general problem of elucidating molecular structures in solution for medium-sized molecules has been met in the last decade by using nuclear magnetic resonance NOE effects. These can be advantageously used to extract interatomic distances, and therefore molecular conformations, but can be of common applicability to rigid molecules only. Two-dimensional nuclear Overhauser effect spectra [1] in the laboratory (NOESY) and rotating (ROESY) frames have proved to be more suitable methods for determining interatomic distances in solution [2–5], and hence molecular structures.

In peptides the intermediate rate of overall motion (around one nanosecond for spherical molecules) can make the NOE in the NOESY spectra vanishingly

Abbreviations: NOESY, nuclear Overhauser enhancement spectroscopy; ROESY, rotating frame Overhauser spectroscopy.

Address for correspondence: Prof. Livio Paolillo, Department of Chemistry, University of Naples, via Mezzocannone 4, 80134 Naples, Italy. Tel. ++39-81-5476530; Fax. ++39-81-5527771; e-mail Paolillo@chemna.dichi.unina.it

CCC 1075-2617/96/010003-11

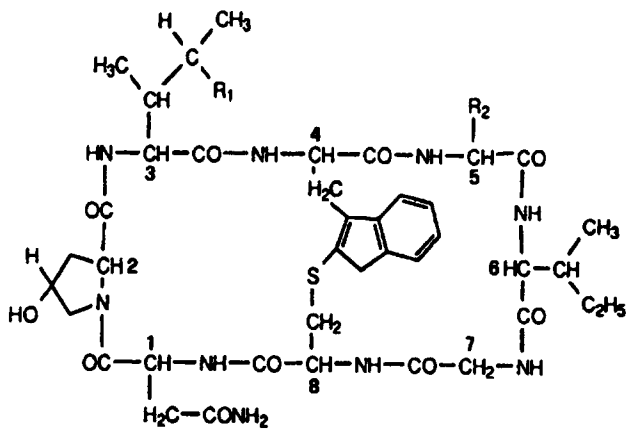

I: R_1=OH, R_2=H

II: R_1=H, R_2=CH_3

III: R_1=H, R_2=H

Figure 1 General chemical structure of amatoxins.

small [1, 4, 5]. ROESY spectra are, then, used to extract interatomic distances from NOE effects in the rotating frame. In medium-sized peptides another possibility arises from the combined use of NOESY and ROESY spectra. From them the accurate evaluation of correlation times [6, 7] becomes possible and therefore the accuracy of calculated distances increases. This is particularly important when molecules belonging to the same family and exhibiting conformational rigidity manifest different biological properties. In the class of amatoxins, amanitins are bicyclic peptides that inhibit *in vivo* the synthesis of DNA-dependent messenger RNA polymerase form II. Several amanitins, both natural and synthetic (Figure 1), have been shown to possess quite similar structures in solution and in the solid state [8] but different [9–11] biological properties. Many attempts to understand the conformational features essential for biological activity by analogue synthesis have not clearly indicated changes in the ring structure when the biological activity is enhanced or decreased. The correct definition of the ring structure is then essential for speculating on the structure–activity relationship. In this paper we present a detailed study on the evaluation of interatomic distances in three amatoxin analogues and their use in molecular dynamics calculations in order to obtain a full characterization of the backbone structure. The first analogue (I) is the biologically active S-deoxo γ[R] OH-Ile^3-amaninamide (Figure 1) that has recently been characterized in the solid state [8] but not in solution. The second analogue (II) replaces a Gly residue in position 5 with an L-Ala residue and is biologically inactive. The third molecule (III) is substituted with a D-Ile in position 3 and is inactive, too. Solution studies made essentially via 2D NMR showed that the first two compounds possess very close conformational features [8, 10]. For the inactive analogue (II) small backbone conformational changes have been suggested and therefore an accurate evaluation of interatomic distances can help in understanding its different biological behaviour. Conformation of compound III is unknown. Considering the bicyclic nature of these molecules, differences in backbone interatomic distances may be quite small. We have, then, first addressed the question of the size of the error involved in the distance evaluation from the NMR data [12]. In this work, the experimentally measured distances were used in restrained molecular dynamics calculations to simulate the structure of the three molecules and their dynamic properties in solution. A detailed account of the results that lead to a full description of the backbone structures is presented.

MATERIALS AND METHODS

NMR Analysis

The synthesis of the S-deoxo γ[R] OH-Ile^3-(I), S-deoxo-Ile^3-Ala^5-(II) and S-deoxo-D-Ile^3 (III) amaninamides is described elsewhere [9, 10]. Two NMR samples for each analogue were prepared by dissolving about 8–9 mg and 2 mg of material in 0.5 ml of dimethylsulphoxide-d_6 (DMSO-d_6) (C. Erba product 99.95% isotopic purity). NMR tubes were sealed before use.

NMR measurements were carried out on a Bruker AM 400 instrument located at the Centro Interdipartimentale di Ricerche di Metodologie Chimico Fisiche and on a Varian Unity 400 located at the Centro Interdipartimentale di Ricerca su Peptidi Bioattivi of the University 'Federico II' of Naples.

Proton and carbon spectra were assigned from homonuclear and heteronuclear 2D correlated experiments. Two series of seven-proton NOESY and six-proton ROESY experiments with mixing times

ranging from 30 to 800 ms were acquired for each analogue. From these experiments peak volumes were measured.

The transformed 2D spectra were baseline corrected before measuring cross- and diagonal peak volumes. The cross-peak volumes were normalized with respect to the diagonal peaks. The frequency offset effect [6] was also corrected for in the case of peaks distant from the carrier frequency. The normalized intensities (A_i) give a linear build-up for small mixing time values up to 0.3 s. The cross-relaxation rates σ_{ij} were calculated from the slope of the build-up curves [2–7]. The same procedure was used for both NOESY and ROESY spectra.

Internuclear distances were calculated from the cross-relaxation rates using the method described in [6].

Molecular Dynamic

The GROMOS package [13, 14] was used for the molecular dynamics calculation. Standard building blocks were used for all residues with the exception of 4-hydroxyproline where the chirality of the γ-carbon had to be reversed from that available in the GROMOS library. A total of 17, 16 and 18 distance restraints from NOE data for analogues I, II and III, respectively, were used. They were introduced twice as lower and upper bounds in a harmonic potential function with a force constant of 1000 and 4000 kJ nm^{-2} mol^{-1} [15]. Distances between geminal protons were neglected as they do not carry any information about dihedral angles. The sulphur–carbon bond between Cys and Trp residues was treated as six additional restraints, but with a force constant 1000 times as tight in order to keep the two groups close in space. The van der Waals repulsions between these two atoms were switched off to simulate the presence of an atomic bond.

Several different trajectories were calculated for each peptide starting from a different initial velocity distribution. For analogue I, the ϕ angles were restrained in five of the eight trajectories according to the coupling constant information. A force constant of 5 or 10 kJ nm^{-2} mol^{-1} was used.

To reduce the number of van der Waals interaction pairs considered in the energy minimization runs, interactions were neglected when the atomic separation became greater than 0.8 nm. Bond length constraints were applied by using the SHAKE algorithm [16, 17]. The system was weakly coupled to a thermal bath of $T = 300$ K with a temperature relaxation time of 0.01 ps during the first 2 and 0.1 ps for all following runs. The initial velocities for the atoms were taken from a random Maxwellian distribution at 300 K. Unique stereospecific assignment for β protons was achieved by using pseudo-atoms (with a 0.1 nm correction) for the first 10 ps to leave the groups flexible to find the best rearrangement. Real atoms were used thereafter. Each MD trajectory covered a period of 51 ps, but only the last 40 ps, when the molecule reached an equilibrium, were considered.

The criterion used for hydrogen bonding was a hydrogen-acceptor distance shorter than 2.5 Å and a D—H···A angle larger than 135°. All calculations were carried out on the VAX 8650 computer of the EMBL in Heidelberg (Germany).

RESULTS

A method used for evaluating interatomic distances r for a two-spin system is based on the measurement of either the cross-relaxation rates in the laboratory σ^n or in the rotating frame σ^r that are both functions of the interspin distance r and of the correlation time τ_c [1]. The correct estimate of τ_c is, therefore, crucial for the proper calculation of r. It has been shown that the combined use of σ^n and σ^r for a given spin pair allows a quite simple estimate of τ_c from Eq. (1) [6, 7, 12]:

$$S(\tau_c) = \sigma^n/\sigma^r = \frac{(5 - 4\omega_o^2\tau_c^2)(1 + \omega_o^2\tau_c^2)}{(1 + 4\omega_o^2\tau_c^2)(5 + 2\omega_o^2\tau_c^2)} \qquad (1)$$

where ω_o is the spectrometer frequency (in radians) and τ_c the correlation time (in s/rad) respectively. $S(\tau_c)$ varies from $-\frac{1}{2}$ to $+1$ in going from $\omega_o\tau_c \gg 1$ to $\omega_o\tau_c \ll 1$. This obviously sets a limit to the applicability of $S(\tau_c)$ which is then meaningful only for τ_c values in the nanosecond range and, in our case, for a spectrometer working at 400 MHz, in the range 0.04–4 ns. In this intermediate range, then, $S(\tau_c)$ depends on τ_c and can be used for its estimate [12].

The general problem of the rational evaluation of correlation times and internuclear distances, the range of applicability of this method and the relative propagation of experimental errors have been described in a previous paper [12]. This method was applied to six geminal $\beta\beta'$ protons belonging to six out of eight amino acid residues in the S-deoxy- Ile$^3\gamma$-OH amaninamide molecule (I) (Figure 1). Because of the intrinsic rigidity of this peptide, the isotropic motion of a rigid body was assumed.

Cross-relaxation rates were independently measured from NOESY and ROESY build-up curves of the cross-peak volumes in the 2D maps. From them, the $S(\tau_c)$ value and the average correlation time τ_c were computed. Although NOE cross peaks in the NOESY spectrum were rather weak, the combined use of this information with the stronger ROEs yields a set of data that can be statistically averaged, thus producing a reliable value of the correlation time.

The relative errors $\Delta S(\tau_c)/S(\tau_c)$ and $\Delta t_c/\tau_c$ are 0.24 and 0.32 as estimated from the error propagation analysis reported in [12]. It is of interest to verify that the average $S(\tau_c)$ value coincides with the value of -0.32 found for geminal $\beta\beta'$ protons. This shows that molecular motions remain essentially constant for all α and β protons and that the rigidity of the bicyclic framework does not significantly change in going from the backbone protons to the side-chain β-protons. The NOE effects with β-protons can therefore be safely used to extract internuclear distances by using the average τ_c value of 0.94 ns. This value is comparable to the correlation time of 1 ns measured from ^{13}C relaxation times at two different magnetic fields.

This method can then be extended to all other spin pairs in the sequence in order to get the structural data necessary for building up a consistent molecular model. Internuclear distances were computed from the cross-relaxation rates in the rotating frames σ^r that were proved to be more reliable for correlation times in the nanosecond range [12].

A similar approach was followed for the other analogues.

Analogue I (*S*-deoxy γ(R) OH-Ile^3-amaninamide)

Chemical shifts for analogue (I) are presented in Table 1. Amide proton temperature coefficients show low values for Asn^1 (−2.3 p.p.b./K), Ile^3 (−0.2 p.p.b./K) and Gly^5 (−1.9 p.p.b./K). A comparison with other similar analogues [9–11] shows large similarities which are representative of rather similar structures for the whole family.

In Table 2 NMR internuclear distances, calculated as described elsewhere [12], are compared to the solid-state distances [8]. Considering that distances in solution are affected by a relative error ($\Delta r/r$) of 0.04, all distances are relatively similar with the exception of the Ile^3 NH-αCH that results slightly shorter (2.60 versus 3.01 Å). A few other distances show deviations that fall outside the estimated average error of 4%. These few cases involve the Ile^6 NH-Gly^5 αCH and mostly distances between α and β protons as in the case of Asn^1. Different conformer populations around the α–β bonds may well account for such differences.

The crystallographic coordinates provided the initial structure for MD simulations. A set of 40 distances was applied to restrain the trajectory. Nine

Table 1 Proton Chemical Shifts δ (p.p.m.) of Analogues I, II and III in DMSO at 298 K. All Chemical Shifts Refer to Internal TMS[a]

		I	II[b]	III
Asn^1	NH	8.50	8.40	8.16
	αCH	4.69	4.90	4.87
	ββ′CH$_2$	3.24; 2.91	3.32; 3.21	2.70 (R); 2.45 (s)
	CONH$_2$	8.13; 7.49	7.47	6.86; 7.26
Hyp^2	αCH	4.40	4.40	4.74
	ββ′CH$_2$	2.20; 1.83	2.44; 2.00	2.06; 1.91
	γCH	4.41	4.57	4.46
	γOH	5.27	5.51	5.32
	δδ′CH$_2$	4.15; 3.72	3.94; 3.48	3.62
Aaa^3	NH	7.94	8.45	8.53
	αCH	4.23	4.50	4.29
	βCH	1.82	2.22	2.10
	γCH	3.76	1.52	1.20
	γ-H	4.51 (γOH)	1.27 (γCH′)	1.20 (γCH′)
	γCH$_3$	1.04	1.03	0.84
	δCH$_3$	0.85	0.98	0.80
Trp^4	NH	8.08	7.83	8.13
	αCH	4.83	5.50	4.90
	ββ′CH	3.29; 3.07	3.30; 3.15	3.67 (R); 2.82 (s)
	4′H	7.01	7.77	7.53
	5′H	7.11	7.17	7.03
	6′H	7.25	7.27	7.12
	7′H	7.58	7.41	7.26
	NH$_{ind.}$	11.26	—	11.23
Aaa^5	NH	8.14	7.63	7.72
	αα′CH	4.28; 3.38	4.27	3.96; 3.54
	βCH$_3$		0.66	
Ile^6	NH	8.50	8.86	8.60
	αCH	3.70	3.95	3.81
	βCH	1.55	1.70	1.64
	γγ′CH$_2$	1.10	1.52; 1.25	1.52; 1.13
	γCH$_3$	0.78	0.92	0.80
	δCH$_3$	0.82	0.92	0.80
Gly^7	NH	8.86	9.13	8.85
	αα′CH	5.91; 3.34	4.10; 3.53	3.94; 3.50
Cys^8	NH	8.06	8.01	7.59
	αCH	4.56	4.71	4.62
	ββ′CH	3.09; 2.87	3.38; 3.10	3.31; 2.96

[a] Aaa^3 refers to D-Ile^3 for analogue III and L-Ile^3 for analogue I and II, and Aaa^5 represents a Gly residue for analogues I and III, and an Ala residue in the analogue II.
[b] These values have been published elsewhere (see [10]).

Table 2 Interproton Distances from 2D ROESY Spectra for Analogues I, II and III and Comparison with X-ray Data (r^X) for Analogue I

	r^X	r^I	r^{II}	r^{III}
Asn^{1}βCH-β′CH	1.75	1.9		
Hyp^{2}βCH-β′CH	1.75	1.9	1.9	
Trp^{4}βCH-β′CH	1.75	2.0		1.9
Cys^{8}βCH-β′CH	1.75	1.9		2.0
Aaa^{5}αCH-α′CH	1.75	1.8		
Gly^{7}αCH-α′CH	1.75	1.8		
Gly^{7}NH-Cys^{8}NH	2.62	2.6	2.7	2.6
Asn^{1}NH-Aaa^{5}NH	2.40	2.7	2.4	
Asn^{1}NH-Cys^{8}NH	2.69	2.7	2.7	
Aaa^{3}NH-Trp^{4}NH			2.4	2.7
Trp^{4}NH-Aaa^{5}NH				2.6
Asn^{1}NH-αCH	2.89	2.5	2.6	
Aaa^{3}NH-αCH	3.01	2.6		
Ile^{6}NH-αCH	2.81	2.9	2.8	3.1
Gly^{7}NH-αCH	2.97	2.8		3.5
Gly^{7}NH-Ile^{6}αCH	2.11	2.1	2.1	2.2
Ile^{6}NH-Aaa^{5}αCH	2.67	3.0	2.4	2.8
Ile^{6}NH-Aaa^{5}α′CH				2.8
Aaa^{3}NH-Hyp^{2}αCH				2.2
Trp^{4}NH-βCH				2.6
Ile^{6}NH-βCH	2.33	2.4	2.4	2.6
Aaa^{3}NH-βCH	2.30	2.4		
Ile^{6}NH-Aaa^{5}βCH			2.7	
Asn^{1}NH-Cys^{8}βCH	2.05	2.5		
Asn^{1}NH-Cys^{8}β′CH	3.60	3.1		
Aaa^{5}NH-Trp^{4}βCH				3.2
Asn^{1}αCH-βCH	2.41	2.5		
Asn^{1}αCH-β′CH	2.45	3.0	3.1	
Hyp^{2}αCH-βCH				2.7
Hyp^{2}αCH-β′CH				3.7
Aaa^{3}αCH-βCH				2.5
Trp^{4}αCH-β′CH				2.5
Cys^{8}αCH-β′CH				2.7
Asn^{1}αCH-Cys^{8}βCH			2.5	
Asn^{1}αCH-Hyp^{2}δCH	2.25	2.2	2.4	
Trp^{4}αCH-4H′	2.34	2.3	2.4	2.4
Trp^{4}βCH-4H′				2.9
Hyp^{2}β′CH-γCH			3.0	
Hyp^{2}γCH-Aaa^{3}βCH			3.0	

[a] All the distances are reported in angstroms. Aaa^3 refers to D-Ile^3 for analogue III and L-Ile^3 for analogue I and II, and Aaa^5 represents a Gly residue for analogues I and III, and an Ala residue in analogue II.

trajectories were calculated starting from different random distributions of velocities and changing the protocol slightly. Three trajectories were calculated using only distance restraints. Five included both distance and angle restraints from coupling constants. A survey of the internal total energies is shown in Table 3. The values obtained are comparable for all the structures.

Table 3 Energy Contributions at Different Stages of the Refinement[a]

	E_{pot}	E_{elec}	ELJ	E_{res}	E_{dih}
Initial	$>10^5$	−202	$>10^5$	201	
After EM	−157	−217	−77	23	
AMa	−58	−228	−76	18	
AmaEM	−203	−236	−87	15	2.3
AMb	−51	−229	−66	17	
AMbEM	−206	−245	−73	13	0.7
AMc	−55	−229	−67	16	
AMcEM	−191	−238	−75	11	3.1
AMl	−45	−236	−56	16	0.8
AMlEM	−206	−245	−74	11	0.8
AMm	−46	−237	−62	22	0.3
AMmEM	−213	−245	−84	15	0.3
AMn	−46	−233	−58	17	0.7
AMnEM	−211	−244	−77	15	0.7
AMo	−46	−237	−62	19	0.6
AMoEM	−201	−245	−81	16	0.6
AMz	−19	−234	−57	34	0.6
AMzEM	−202	−245	−73	11	0.6

The trajectories differ by the choice of the initial velocities using the following protocol: 1 ps at 300 K and τ (the thermal coupling constant) = 0.01, 50 ps at 300 K and $\tau = 0.1$. The first three trajectories were run without dihedral angle restraints and with a force constant for distance restraints of $K_{res} = 1000$ kJ nm^{-2} mol^{-1}. Dihedral angle restraints were added to the trajectories identified by AMl, AMm and AMn with a force constant of $K_{dih} = 5$ kJ deg^{-2} mol^{-1}. The last two trajectories were obtained by increasing K_{dih} to 10 kJ deg^{-2} mol^{-1} (AMo) and, in addition to this, K_{res} to 4000 kJ nm^{-2} mol^{-1} (AMz). One-thousand cycles of energy minimization using the conjugated gradient algorithm were applied to the final snapshots obtained from the dynamics. A K_{res} of 1000 kJ nm^{-2} mol^{-1} and a K_{dih} of 5 kJ deg^{-2} mol^{-1} were used.

The final snapshots from the dynamics obtained after the final energy minimization are shown in Figure 2. The averaged structure is compared with the solid-state structure in Figure 3. The average r.m.s. deviation between structure pairs is 0.59 for the backbone atoms (N, αC, C). The average r.m.s. deviations from the X-ray structure for the backbone atoms are 0.59 and 0.74 Å including the oxygens, and 1.10 Å for all the heavy atoms (excluding the hydrogens). This shows that the solution structure is relatively close to that observed in the crystal state. The main differences are located in the orientation of the side chains and of the carbonyl oxygen atoms so that the ϕ, ψ angles can differ, but without any substantial change of the overall 3D shape (Table 4).

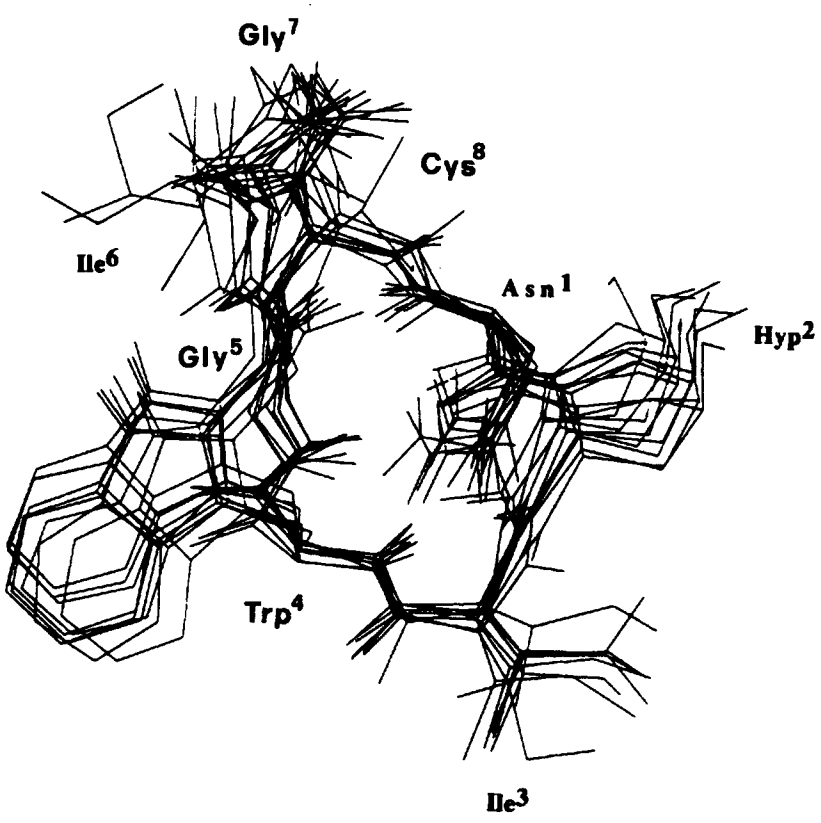

Figure 2 Stereoview of the superposition of the eight final snapshots after 51 ps of MD for analogue I.

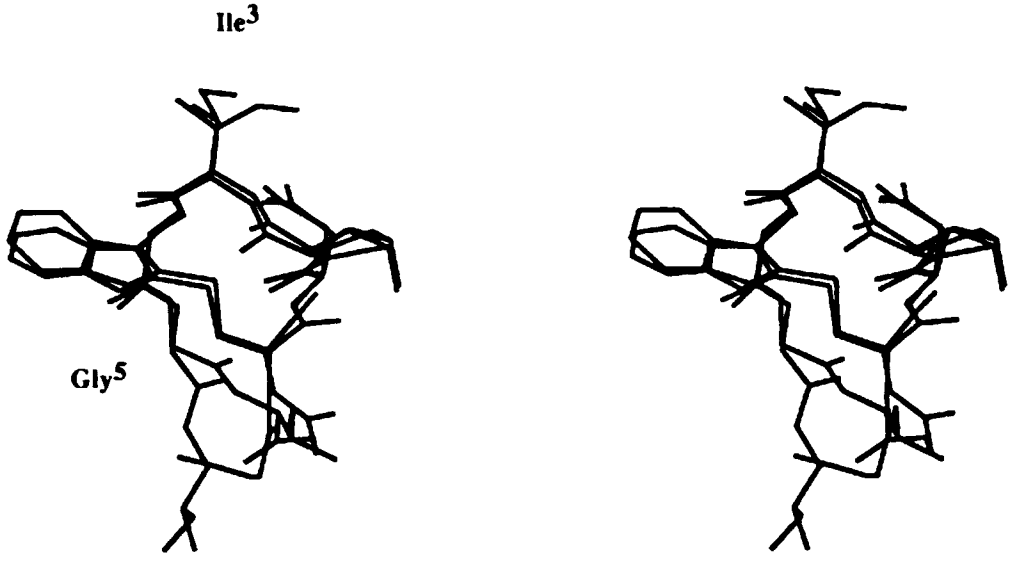

Figure 3 Stereoview of the superposition of the averaged structure obtained from MD and X-ray structure for analogue I.

Table 4 ϕ, ψ and χ Dihedral Angles Obtained from MD Simulations for all Analogues. For Analogue I, ϕ and ψ angles from the X-ray structure [8] are Reported

	ϕ	ψ	χ_1	χ_2	ϕ (RX)	ψ (RX)
Analogue I						
Asn[1]		159.6	62.7	72.7	−163	180
Ile[3]		−43.9	−48.4		−98	−32
Trp[4]	−76.8	−3.2	178.9	−119.7	−93	−23
Gly[5]	111.6	138.7			114	−166
Ile[6]	−57.9	139.4	−58.4		−52	136
Gly[7]	96.1	−46.4			−80	0
Cys[8]	−75.2		−178.3		−131	−88
Analogue II						
Asn[1]		160.2	65.1	75.9		
Ile[3]		−55.3	−64.7			
Trp[4]	−89.3	54.8	179.7	−112.8		
Ala[5]	52.4	−171.4				
Ile[6]	−58.3	136.2	−53.5			
Gly[7]	87.1	−37.7				
Cys[8]	−87.3	0	178.9			
Analogue III						
Asn[1]		155.3	60.1	42.9		
Trp[4]		−25.9	161.4	−116.3		
Gly[5]	80.2	−74.1				
Ile[6]	−59.2	95.4	48.8			
Gly[7]	54.1	43.1				
Cys[8]	−155.0		58.8			

The resulting structure is very compact and looks like a jar with the four long side chains (Ile[3], Ile[6], Hyp[2] and Trp[4]) as handles (Figure 2). If we consider the dispersion of the structures as representative of the conformational space covered by the structures, two motions seem to be dominant: (1) minor motions of the carbonyl groups around the backbone, so that the ϕ/ψ angles may change slightly without major conformational changes; (2) higher mobility is shown by the side-chains, especially at Ile[6], and, to a minor extent, at Ile[3]. The position of the Hyp[2] ring as a whole moves in space. The orientation of the Trp ring is relatively fixed in space. A hollow region divides this ring from Gly[5]. Five hydrogen bonds are common to the X-ray structure. Two of them are bifurcated bonds: one links the Gly[5] carbonyl with the Asn[1] and Cys[8] amide protons, the other binds Asn[1] side-chain carbonyl and Trp[4] and Ile[3] amide protons. Together with a hydrogen bond between Gly[5] amide proton and Asn[1] carbonyl, they confer rigidity and compactness to the structure. In addition, two hydrogen bonds between the side-chain NH_2 group in Asn[1] and the Cys[8] carbonyl group, and the amide proton in Cys[8] and the Ile[6] carbonyl may form in solution with low occupancy.

Analogue II (*S*-deoxo-Ile[3]-Ala[5]-amaninamide)

Relevant NMR parameters (chemical shifts, coupling constants and amide proton temperature dependences) for analogue II have been published elsewhere [10] and some of them are reported in Table I. Distances have been measured with the method outlined for analogue I. All distances are strikingly similar, but for Ile[6] NH-Ala[5] αCH, within the limits of estimated deviations. Coupling constants are also very similar in the two analogues [10]. As similar structures lead to similar experimental observables, especially in such highly constrained molecules, we can therefore confidently assume that despite the amino acid substitution in position 5 and the minor variations of the Trp[4] and Ala[5] ϕ and ψ angles, no significant conformational changes can be envisaged between the two analogues.

It is important to consider that this analogue possessing an L-Ala residue in position 5 is inactive, while the corresponding D-analogue is, in contrast, active. Previous conventional NMR studies [10] have failed to recognize substantial conformational changes and it was postulated that a possible cause of biological inactivity lies in the perturbation of the tryptophan indole ring accessibility.

Internuclear distances can clearly help in building up a molecular model that demonstrates this hypothesis. NOE effects and cross-relaxation rates measured from both NOESY and ROESY 2D spectra yield an average $S(\tau_c)$ value of -0.25 which is quite similar to that of -0.32 found for analogue I. The calculated average correlation time of 0.81 ns is again consistent with the previous finding. Calculated internuclear distances are reported in Table 2 where they are compared with the other analogues. The reported $\beta\beta'$Hyp distance of 1.9 Å is in line with that found in analogue I, thus confirming the reliability of the method. All other calculated distances are strikingly similar within the limits of the estimated deviations. Despite the amino acid substitution in position 5 the structures then appear identical. Molecular dynamic calculations based on the NOE restraints permit a model of this analogue in solution to be built (Figure 4). R.m.s. deviations of analogues I and II differ by 1.2 Å and their structures appear almost superimposable (Figure 4), thus confirming the hypothesis based on the NMR parameters [10]. The only important structural differ-

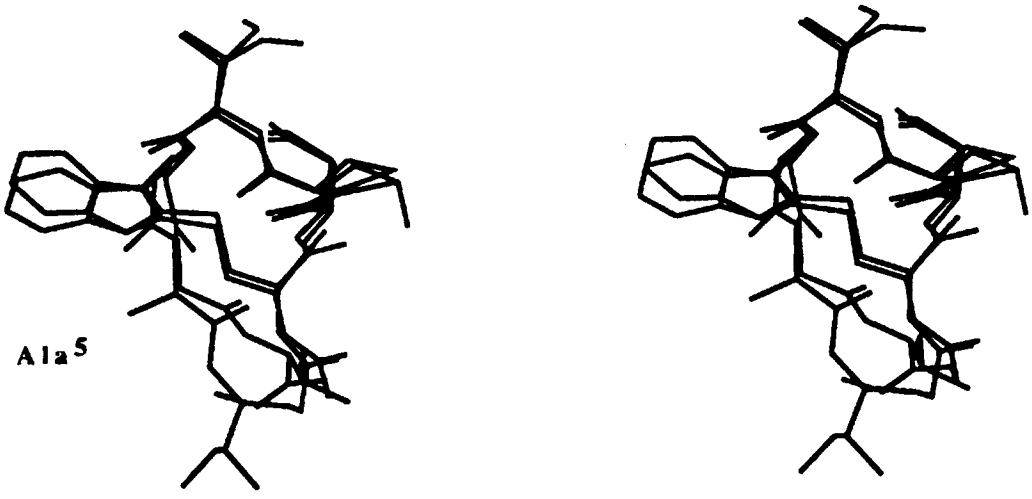

Figure 4 Superposition of the MD structures of analogue I and analogue II. According to the analysis the structure of the two analogues is very similar. The accessibility of the Trp ring is, however, strongly reduced in analogue II by the presence of methyl in the L-amino acid.

ences lies in the L-Ala^5 methyl group pointing toward the Trp^4 ring, suggested earlier as a possible cause of inactivity. If we consider the plane defined by the backbone of residue 5, the methyl group points to an axial position parallel to the tryptophan ring. This would not cause changes in the conformation since there is room enough to accommodate an even bulkier side chain, but would prevent a possible interaction of Trp^4 with the receptor. The D-Ala^5 analogue, in contrast, with its methyl group pointing equatorially away from the ring should retain its activity. Indeed experiments carried out on the D-Ala^5 analogue prove that it is active [10]. It can be concluded that this inactive analogue does maintain the backbone structure of the active amatoxins. The reason for the *in vitro* lack of activity is, then, not due to conformational differences but is to be found in the side-chain tryptophan orientation, probably masked by the alanine methyl group, thus disfavouring any active interaction at the biological site.

Analogue III (*S*-deoxo-D-Ile^3-amaninamide)

Chemical shifts, from 1D and 2D NMR experiments at 298 K, are reported in Table 1. The temperature dependence of the amide protons shows low values of the temperature coefficients of Asn^1 (−1.0 p.p.b./K), γ'NH Asn^1 (−0.3 p.p.b./K), Gly^5 (−0.4 p.p.b./K) and Cys^8 (−0.9 p.p.b./K), thus indicating that they are not exposed to the solvent and are possibly involved in intramolecular hydrogen bonds.

Figure 5 Superposition of the MD models for analogues I and III.

Interproton distances for analogue III have been evaluated according to the method used for the other analogues. In Table 2 the distances calculated according to the estimate of the correlation time τ_c are reported. The average τ_c value is 0.94 ns, which agrees with those estimated for the other two analogues.

NOE restraints have been used in the MD calculations for building a plausible model for this analogue. The results are presented in Figure 5 where the calculated structure is compared with that of analogue I. In addition, in Table 4 the ϕ and ψ angles for all three analogues, as obtained from the MD simulations, are reported.

Figure 5 shows the structure of analogue III superimposed on that of analogue I (Gly^5, L-Ile^3). It is clear that the two structures are quite different. If the segment Trp^4-Ile^3-Asn^1-Cys^8 is kept superimposed (as in Figure 5), the rest of the molecule in analogue III is oriented in a completely different way. This is further proved by examining the ϕ and ψ torsion angles in Table 4 where analogue III shows larger deviations in comparison to the other analogues.

DISCUSSION

In this paper we have met the problem of the accurate determination of the conformational features of three substances (amatoxins) that are known to be of bicyclic nature and of low molecular size and therefore to have a rigid structure as far as the backbone is concerned. It is also known that the biological activity of the three amatoxins is not retained when the Gly in position 5 is substituted with an L-Ala residue or when the L-Ile in position 3 is replaced by a D-Ile residue. The aim of the present work is then to identify the reasons for such inactivity, whether conformational, configurational or both. We demonstrate that the combined use of NMR techniques and molecular dynamics is a valid methodology to solve this problem. In all cases the chirality of the thioether bridge has been determined to be the same, i.e. of the P-type [18, 19]. Amanitin analogue II with an L-Ala residue in position 5 has the backbone structure in solution quite similar to that found in the solid state (Figure 1) for the natural toxic molecule. The different orientation of the amino acid side chains observed in the averaged solution structure cannot be considered responsible for the biological inactivity of this analogue, considering that little energy is required for a position reorientation in the interaction with the enzyme (RNA-polymerase). Then, the hypothesis that in the tryptophan ring full accessibility is an important structural element for the biological activity gains strength and validity and gives definitive support to the previous NMR study [10].

The tenfold biological activity decrease of analogue II can thus be considered of configurational origin with the methyl group of L-Ala residue masking the tryptophan ring. This conclusion agrees with studies carried out on a number of natural and synthetic analogues. It is in fact well established that the indole ring is an important structural element in the recognition site of the enzyme [20]. Any perturbation

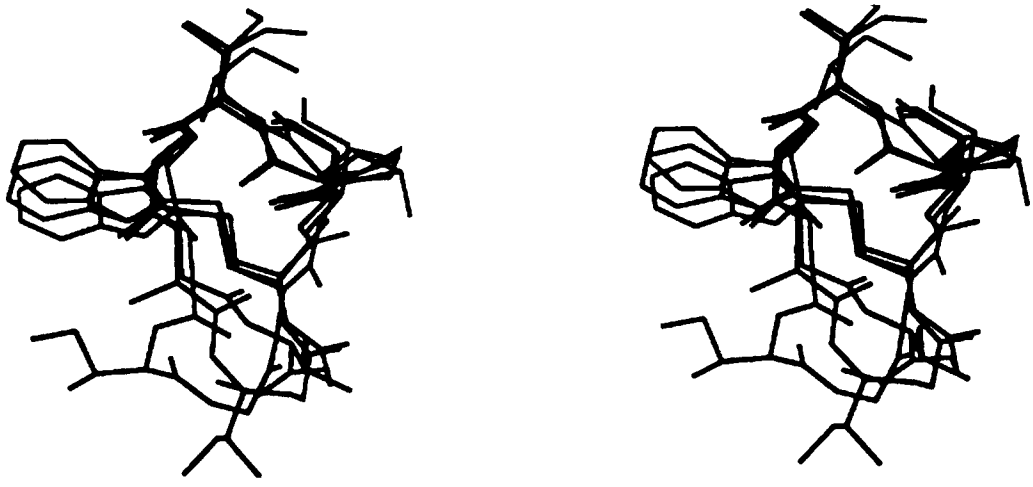

Figure 6 Superposition of the MD models for all analogues.

of the indole ring accessibility then decreases the active orientation within the active site, thus reducing the biological activity.

The case of analogue III is, however, quite different. ϕ and ψ angles (Table 4) calculated with dynamic simulation demonstrate that the backbone ring structure is distorted when compared with the native one. As a consequence, the inactivity of this analogue can be confidently ascribed to the different ring conformation that makes any active coupling with the enzyme impossible. This is clearly presented in Figure 6 where the analogue III conformation is superimposed on those of the other two analogues. While analogues I and II are rather similar as far as the backbone structure is concerned, analogue III shows a quite different backbone conformation. Therefore, the preferential orientation of the structural elements relevant to the activity is missing and, as a consequence, this analogue is totally inactive.

In conclusion, it is legitimate to state that in the case of rigid molecules with cyclic peptide frameworks, NMR coupled to theoretical calculations provides a unique tool for careful monitoring of solution conformation.

Acknowledgements

A.L.P. would like to thank Dr G. Vriend for allowing her the use of his graphics program WHATIF.

REFERENCES

1. D. Neuhaus and M. Williamson: *The Nuclear Overhauser Effect in Structural and Conformational Analysis.* VCH Publishers Inc., New York 1989.
2. S. Macura and R. R. Ernst (1980). Elucidation of cross-relaxation in liquids by two-dimensional n.m.r spectroscopy. *Mol. Phys. 41*, 95–117.
3. A. Kumar, R. R. Ernst and K. Wütrich (1980). A two-dimensional nuclear Overhauser enhancement (2D NOE) experiment for the elucidation of complete-proton–proton cross-relaxation networks in biological macromolecules. *Biochem. Biophys. Res. Commun. 95*, 1–6.
4. A. A. Bothner-By, R. L. Stephens, J.-M. Lee, C. D. Warren and R. Jeanloz (1984). Structure determination of a tetrasaccharide: transient nuclear Overhauser effects in the rotating frame. *J. Am. Chem. Soc. 106*, 811–813.
5. A. Bax and D. G. Davis (1985). Practical aspects of two-dimensional transverse NOE spectroscopy. *J. Magn. Res. 63*, 207–213.
6. D. G. Davis (1987). A novel method for determining internuclear distances and correlation times from NMR cross-relaxation rates. *J. Am. Chem. Soc. 109*, 3471–3472.
7. B. T. II Farmer, S. Macura and L. R. Brown (1988). The effect of molecular motion on cross-relaxation in the laboratory and rotating frames. *J. Magn. Reson. 80*, 1–22.
8. G. Zanotti, T. Wieland, E. Benedetti, B. Di Blasio, V. Pavone and C. Pedone (1989). Structure–toxicity relationship in the amatoxin series. Synthesis of *S*-deoxy[γ(*R*)-hydroxy-Ile^3]-amaninamide, its crystal and molecular structure and inhibitory efficiency. *Int. J. Peptide Protein Res. 34*, 222–228.
9. G. Zanotti, G. D'Auria, L. Paolillo and E. Trivellone (1986). Synthetic amatoxin analogue. A two-dimensional proton NMR study of *S*-deoxy-(Ile^3)-(D-Ala^7)-amaninamide. *Biochem. Biophys. Acta 870*, 454–462.
10. G. Zanotti, G. D'Auria, L. Peolillo and E. Trivellone (1988). Synthetic amatoxin analogues. II. A proton n.m.r. study of *S*-deoxo-Ile^3-(L)-Ala^5 and *S*-deoxo-Ile^3-(D)-Ala^5-amaninamide. *Int. J. Peptide Protein Res. 32*, 9–20.
11. G. Zanotti, T. Wieland, G. D'Auria, L. Paolillo and E. Trivellone (1990). *S*-deoxo-Abu^1, Ile^3-amaninamide, an inactive amatoxin analogue. *Int. J. Peptide Protein Res. 35*, 263–270.
12. C. Isernia, L. Paolillo, E. Russo, A. L. Pastore, G. Zanotti and S. Macura (1992). Evaluation of errors of interproton distances and correlation time determined from NMR cross-relaxation rates. *J. Biomol. NMR 2*, 573–582.
13. H. J. C. Berendsen, J. P. M. Postma, W. F. van Gunsteren and J. Hermans in: *Intermolecular Forces.* B. Pullman, Ed., p. 331–342, D. Reidel, Dordrecht 1981.
14. W. F. van Gunsteren, R. Kaptein and E. R. P. Zuiderwerg in: *Nucleic Acid Conformation and Dynamics.* W. K. Olson, Ed., p. 79–92, Report of NATO/CECAM Workshop, Orsay 1983.
15. W. F. van Gunsteren, R. Boelens, R. Kaptein, R. M. Scheek and E. R. P. Zuiderwerg in: *Molecular Dynamics and Protein Structure*, p. 92–99, Polycrystal Book Service, Western Springs 1985.
16. J. P. Ryckaert, G. Ciccotti and H. J. C. Berendsen (1977). Numerical integration of the Cartesian equations of motions of a system with constraints: molecular dynamics of *n*-alkanes. *J. Comp. Phys. 23*, 327–341.
17. W. F. van Gunsteren and H. J. C. Berendsen (1977). Algorithms for macromolecular dynamics and constraint dynamics. *Mol. Phys. 34*, 1311–1327.
18. T. Wieland, B. Beijer, A. Seeliger, J. Dabrowski, G. Zanotti, A. E. Tonelli, A. Gieren, B. Dederer, V. Lamm and E. Hädicke (1981). Components of the green deathcap toadstool (*Amanita phalloides*), LIX. The

spatial structure of Phallotoxins. *Liebigs Ann. Chem.*, 2318–2334.

19. G. Shoham, D. C. Rees, W. N. Lipscomb, G. Zanotti nd T. Wieland (1984). Crystal and molecular structure of *S*-deoxo[Ile^3]amaninamide: a synthetic analogue of *Amanita* toxins. *J. Am. Chem. Soc. 106*, 4606–4615.
20. T. Wieland, C. Gotzendorfer, J. Dabrowski, W. N. Lipscomb and G. Shoham (1983). Unexpected similarity of the structure of the weakly toxic amanitin (*S*)-sulphoxide and the highly toxic (*R*)-sulphoxide and sulfone as revealed by proton nuclear magnetic resonance and X-ray analysis. *Biochemistry 22*, 1264–1271.